Design and Fabrication of Two Heterojunction Devices Performance for Photodetectors Applications

Maysoon Hashim Ismaail[1], Alaa Hussein Ali[2], Sabah M. Thaba[3]

[1,2]Department of Electrical Engineering, University of Technology, Baghdad, Iraq
[3]Nanotechnology and Advanced Materials Research, College of Engineering, University of Kufa, Najaf, Iraq
[1]eee.19.03@grad.uotechnology.edu.iq, [2]alaa.h.ali@uotechnology.edu.iq, [3]Sabah.alabboodi@uokufa.edu.iq

Abstract— Hydrothermal preparations have been made form vanadium oxygen systems V2O5 and VO2 NPs prototype to design photodetectors. In comparison, the films' polycrystalline structure can be seen in analysis of x-ray diffraction (XRD) pattern, which has 7 and 14 peaks with crystallite sizes = 19.59 for V2O5 and, crystallite sizes = 12.92 nm, for VO2. The grains had large, neatly separated conical columnar growth combined grains throughout the surface, with some of the columnar grains coalescing in a few spots, according to the analysis from atomic force microscopy (AFM). It is revealed that the average size of particle of V2O5 =29.58 nm and for VO2 = 16 nm, with rms roughness of 6.8 nm and 21.3 nm respectively. Also, the optical energy gap of V2O5 = 2.6 eV, whereas energy gap of VO2 = 1.36 eV. In addition, it was discovered that the reflectance increased in the visible and infrared regions to register 0.09 and 0.07 respectively. The maximum values of the refractive indices for V2O5 and VO2 were 2.6 and 1.9, respectively. Two types of hetero-junction photo-detectors Ag/VO2/PSi/n-Si/Ag and Ag/V2O5/PSi/n-Si/Ag have been fabricated and characterized. The proposed results of Ag/ V_2O_5 /PSi/n-Si/Ag heterojunction Photo-detector at different concentrations from PMMA: Acetone responsivity was 0.7A/W at 850nm and, the remarkable detectivity = 4.1 x 10^{12} (1/W) .cm. $Hz^{0.5}$, while, highest values of the detectivity in Ag/VO2/PSi/n-Si/Ag = 3.3 x 10^{12} (1/W) .cm.$Hz^{0.5}$ at wavelength equal and greater than 850 nm.

I. INTRODUCTION

The essential class of materials used in a variety of industrial applications, vanadium oxides which, exhibit an intriguing and wide range of chemical and physical properties due to diverse metal oxidation states (from +II to +V) and V-O coordination geometries. For more than 50 years, the theoretical and experimental summarized substance and materials communities have studied vanadium oxygen systems (V2O5, VO2), a model of intensely associated materials [1, 2]. Compared to other vanadium oxides, Vanadium Pentoxide (V2O5) has excellent electronic and chemical properties, making it a possible applicant for electronic applications [3, 4]. V2O5 is a great option for optoelectronic applications like photo-detectors because it has a straight band gap of 2.2 eV to 2.7 eV [5]. Vanadium dioxide (VO2) is a well-known "smart substance" that has become more well-known since the Morin work in 1959. Its monoclinic M1 phase displays a metal-insulator transition (MIT) behaviors near-room-temperature, which increases the requirements for nonmaterial structural. However, reported till date now involve complex structures and constrained wavelength response, and, there is limited understanding of the parameters which, are controlled the insulator-to-metal transition IMT and, the photoresponse in VO_2 photo sensor [5, 6].

In addition, vanadium oxides can have a wide range of V: O ratios, which results in diverse operational styles. Vanadium oxides, VO2, include more than 15 additional stable vanadium oxide phases (such as VO, V2O3, V3O5, etc.), with VO2 and V2O5 being the two most intriguing vanadium oxides [7-9]. Electromagnetic radiation is absorbed by the detector's transducer, which then emits an

electrical signal that is typically related to the radiation's intensity. P-n junctions are commonly found in semiconductor-based photo-detectors, which convert the light photons into output signal can either be a current or a voltage [7-10].And by using crystalline silicon wafers which are electrochemically etched in a hydrofluoric acid-based electrolyte solution under constant anodization conditions like etching time, current density, HF concentration, and Si orientation, porous silicon (PSi) is created. Porous silicon is made up of a network of nanoscale-sized silicon. There are a wide ranges of potential applications for porous silicon structures, including waveguides, 1D photonic crystals, chemical sensors, biological sensors, photovoltaic devices, etc. [11, 13]. Porous silicon structures also have good mechanical robustness, chemical stability, and compatibility with existing silicon technology. In present work design and fabrication two heterjunication photodetectors from V2O5 and VO2 nanoparticles by using a hydrothermal method will be compared and contrasted as well as to investigate the characteristics of the photodetectors. The presence of Vanadium dioxide on the surface produces composites with increased surface area of exposed electrolyte, which ultimately improves electro-optical performance. Implementation and experimental testing use to prepare the characteristics of vanadium dioxide nanostructures and its application for Nano phonics devices. A significant enhancement in photo response of photodetectors could be achieved by optimizing the size of the device and, the substrates type. The broadband photo-response opens opportunities for designing and controlling the performance o for scalable Micro and Nano-scale devices.

II. EXPERIMENTAL PART

A. Materials and Method

Firstly, material V2O5 NPs were created using the hydrothermal method, which involved by adding 1.8 g of powder to 100 ml of distilled water, stirring the mixture for 15 min at 50 oC, letting it cool to room temperature, and then adding 1 g of Poly(methyl methacrylate PMMA to 50 ml of acetone at a concentration of (1.5:8.5) as shown in *Fig. 1*. Secondly, VO2 NPs were made using the hydrothermal method, which involved adding 1.8 g of material powder to 100 ml of distilled water, stirring the mixture for 15 minutes at 50 oC, and then letting it cool to room temperature. Firstly, to prepare the material, 1.5g of Polyvinylpyrrolidone (PVP) was added to 50ml of ethanol. as shown in *Fig. 1*.
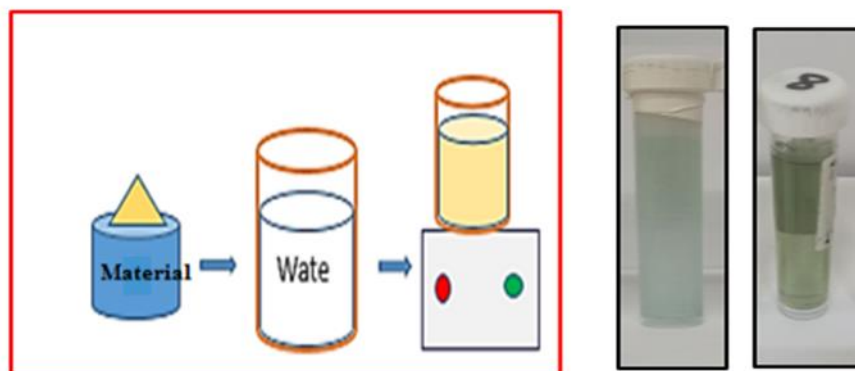

FIG. 1. PREPARATION OF NPS ON THE LEFT DIAGRAM OF HYDROTHERMAL METHOD, IN THE MIDDLE V2O5 ON THE RIGHT VO2.

B. Etching Cell Preparation

A silicon wafer (n-type) was cut into small slides that were (1.5cm * 1.5 cm) in size. The slides were then rinsed in ethanol for 10 seconds to take out dirt and the natural oxide layer from the models. Following cleaning, it is submerged in a mixture of HF (40%) and ethanol (99.99) (1:1) at room temperature. In etching process, a Teflon cell with an Au ring as an electrode was utilized and a Halogen

lamp with a light intensity of (100) mW/m as shown in *Fig. 2*, 10 mA/cm2 current density was useful to use for the duration of (10) min and, to yield an etched area of the model totally around the cell (0.785 cm2).

FIG. 2. PRACTICAL SETUP OF PHOTOELECTROCHEMICAL ETCHING TECHNIQUE.

C. Characterizations of Heterojunction Ag/V2O5/PSi/n-Si /Ag and Ag/VO2/PSi/n-Si/Ag

In order to measure the properties of photo-detectors, thin films of the compounds (V2O5 and VO2) were applied to a PSi slide using the drop casting method, and then Ag electrodes were applied to the top and bottom surfaces and then connected to a circuit as shown in *Fig. 3*. When the light strikes the detector, the photons excited the electrons to higher energy levels lead to the formation of electrical charge carriers (e or h) that remain inside the detector material. This detector converts photons in straight to some free current carriers. For valence electrons to be excited, the incident photon's energy must be equivalent to or bigger than the band gap energy.
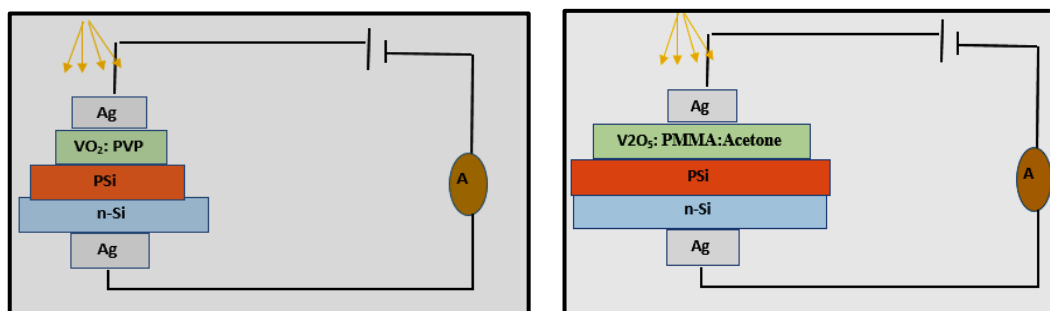

FIG. 3. DIAGRAM CONNECTION CIRCUITS FOR DETECTORS.

III. RESULTS AND DISCUSSION

The comparison between two hetero-junction devices V2O5: PMMA/PSi and VO2: PVP/PSi for Photodetector applications present in this work. *Fig. 4 (a, b)* describe the results of X-ray diffraction for V2O5 and VO2 the thin films that deposited by drop casting method on the glass substrate. It observed that thin films of V2O5 and VO2 are polycrystalline structure, with 7 and 14 peaks respectively. The crystallite size values of V2O5 and VO2films were calculated by measuring by Scherer's equation (21.91 and 11.19) nm respectively[14-17].

$$D = \frac{0.9\lambda}{B \, Cos \, \theta} \qquad (1)$$

Where D is the mean crystallite size, λ is the wavelength of CuKα (=1.5405 Å), B is the full width at half maximum (FWHM) and θ is Bragg's diffraction angle.
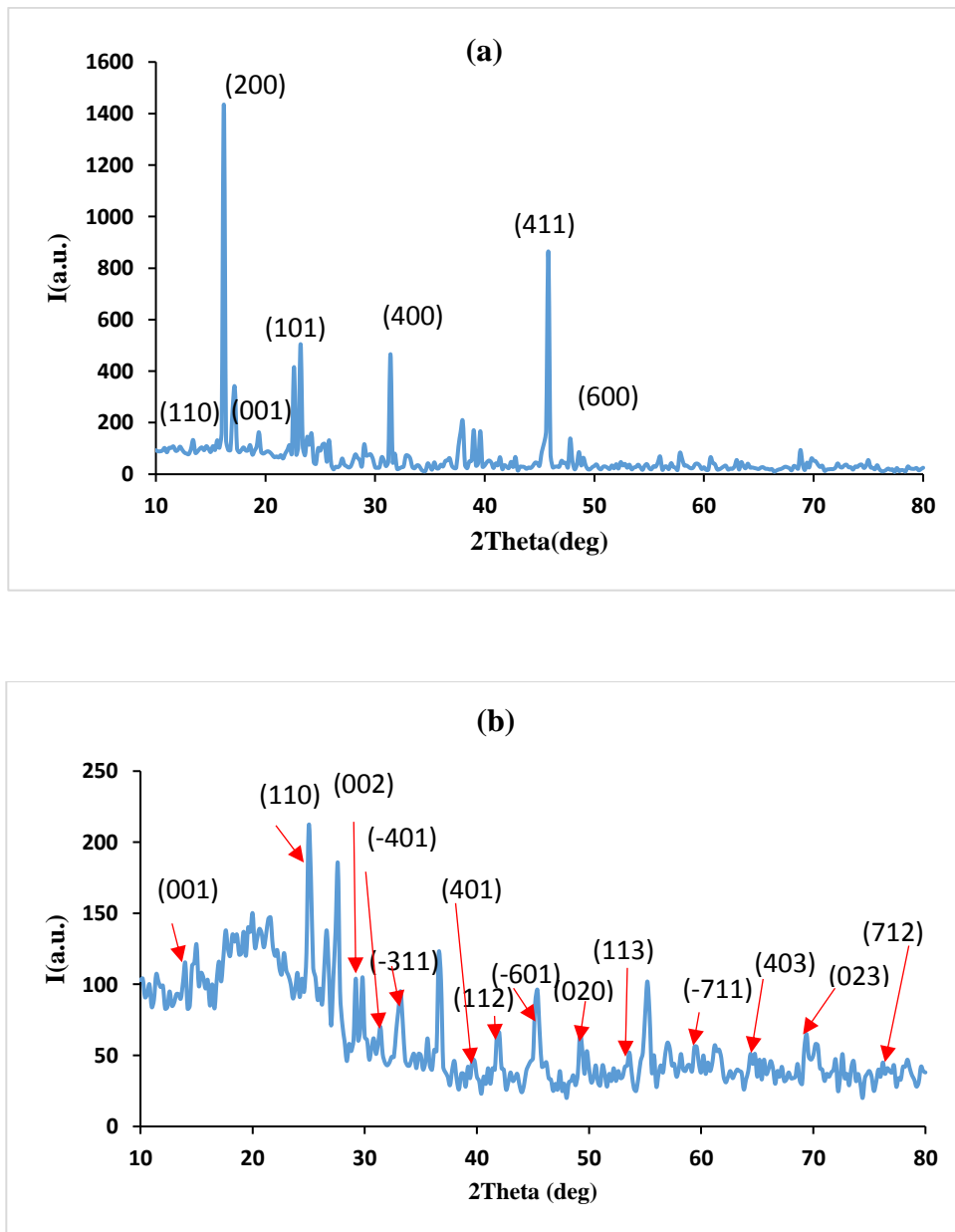

FIG. 4. (A). X-RAY DIFFRACTION FOR V2O5 FILM AND (B). X-RAY DIFFRACTION FOR VO2 FILM.

AFM analysis using atomic force microscopy revealed a porous free morphology with homogeneity and uniformity on the films surface. *Fig*. 5 *(a, b)* displays 3D AFM micrographs and histograms of (V2O5 and VO2). There were no visible cracks on the surface of the film. The grains had large, neatly separated conical columnar growth combined grains all over the surface with some columnar grains coalescing in a few spots. It displayed average particle sizes of 14.3 and 16.4 nm, rms roughness of 6.8 and 21.3 nm, respectively.
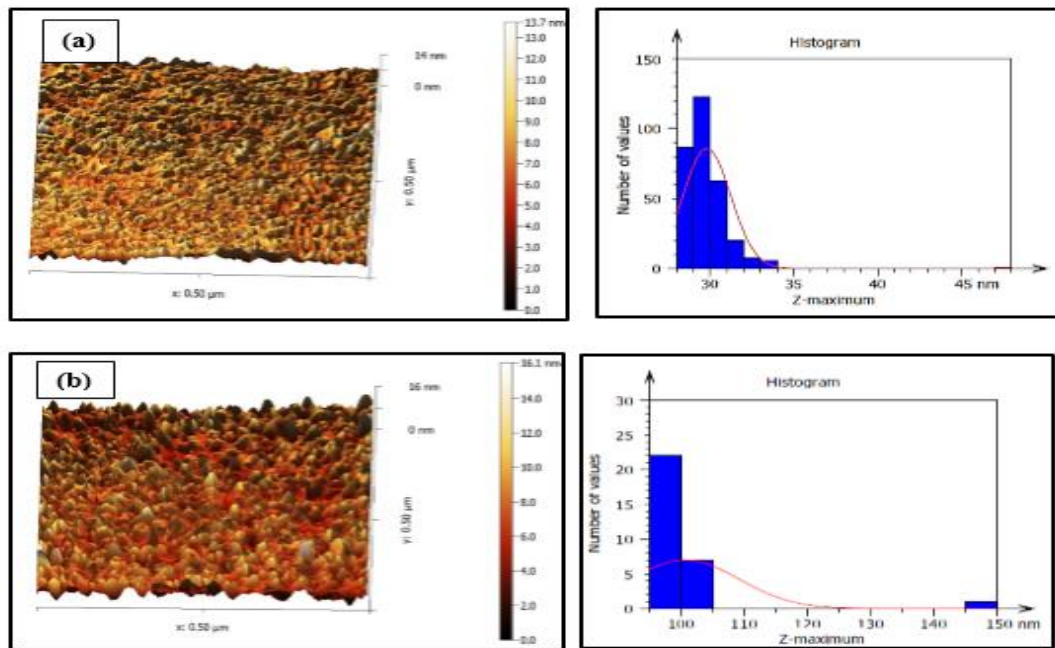
FIG. 5. AFM IMAGE HISTOGRAM OF (A) V2O5 THIN FILM AND (B) VO2 THIN FILM.

The absorption spectra was studied using UV-Visible-Near-Infrared (NIR) spectroscopy at range (200-1100) nm for both samples (V2O5 and VO2). *Fig. 6* shows the UV-Vis-NIR spectrum of films at where its exhibits good absorbance in UV range (200-300 nm) where the transmittance increasing withe increase of wavelength in visible region and IR. The maximum absorbance record 90% and 29% at wavelength 200 nm for V2O5 and VO2 respectively. Energy gap of the films estimated by extrapolating the line, where Eg value was (2.6) and (1.36) eV for V2O5 and VO2 respectively as shown in *Fig. 7* [18, 21].
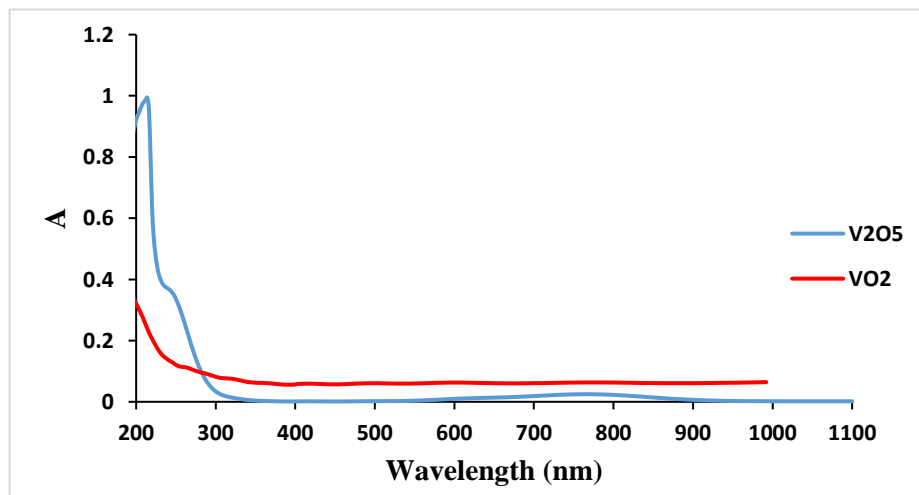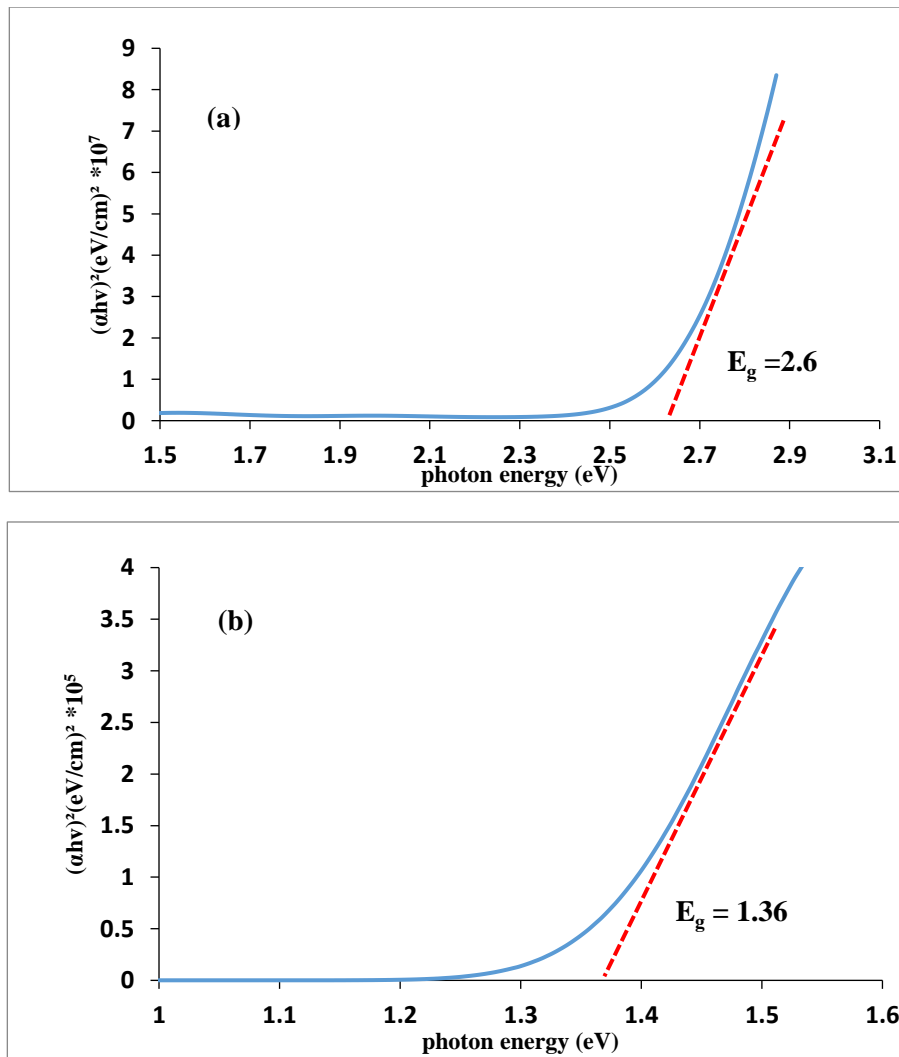

FIG. 6. UV-VISIBLE SPECTRA OF V2O5 AND VO2.

FIG. 7. VARIATION OF $(AHV)^2$ WITH PHOTON ENERGY FOR (A) V2O5 AND (B)VO2.

Fig. 8 displays the samples' reflectance spectra as a function of wavelength in the range (300-1100). reflecting factor calculated using relationship (2)[22]. It is important to note that reflectance values increase in the visible and IR regions and decrease at wavelengths (500nm) to record 0.09 and 0.07 at 780nm. The refractive index is a crucial parameter for semiconductor materials and applications. It depends on a number of variables, including the kind of material and crystal structure, and its values change as the roughness of the sample surface changes. Refractive index as determined by relationship (3) [22]. In the range of wavelengths shown in *Fig. 9*, the refractive indices of V2O5 and VO2 are shown as a function of wavelength (200-1100nm). At a wavelength of 300 nm, the maximum values of the refractive indices for V2O5 and VO2 were 2.6 and 1.9, respectively.

$$R + T + A = 1 \qquad (2)$$
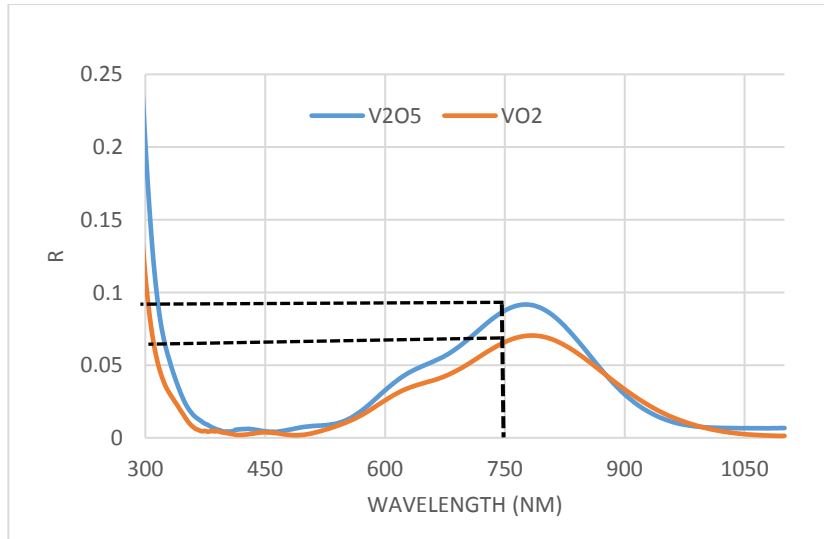
$$n = \frac{1+\sqrt{R}}{1-\sqrt{R}} \qquad (3)$$

FIG. 8. REFLECTANCE SPECTRA OF V2O5 AND VO2.
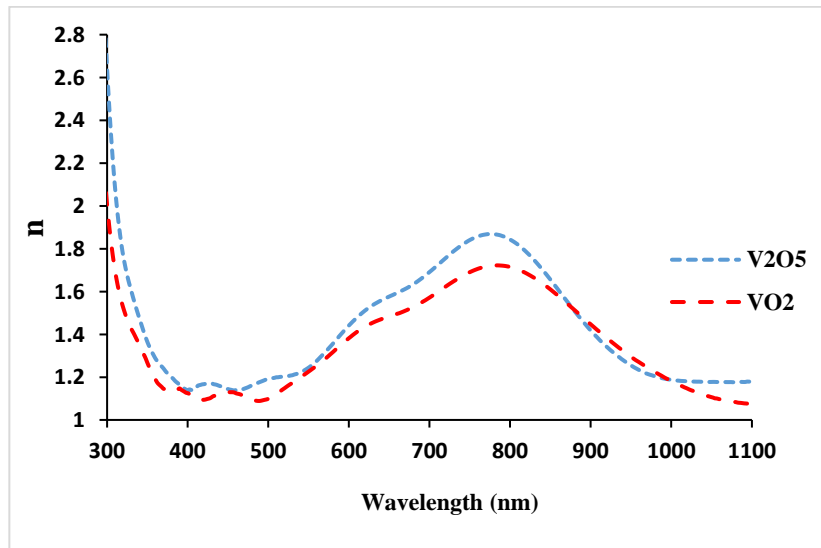
FIG. 9. REFRACTIVE INDEX OF V2O5 AND VO2.

Fig. 10 (a, b) show the spectral responsively as the function of wavelength of Ag/V2O5: PMMA/Psi/Ag and Ag/VO2: PVP /Psi/Si/Ag structures. The spectral responsively calculated from the relationship (4) [23]. It observed from *Fig. 6 a* spectral responsively of structure has consist of 3 peaks located at 460,750 and 852nm due to the absorption of V2O5, Psi and Si respectively. Ag/V2O5: PVP/Psi/Si/Ag structure also has 3 peaks located at 751, 850nm and 920 due to the absorption of Psi, Si and VO2 respectively.

$$R_\lambda = \frac{I_{Ph}}{P_{in}} \quad (A/W) \quad\quad (4)$$

FIG. 10. RESPONSIVELY AS A FUNCTION OF WAVELENGTH OF (A) V2O5: PMMA/PSI/ N- SI PHOTO-DETECTORS AND (B) VO2: PVP/PSI/ N- SI PHOTO-DETECTORS
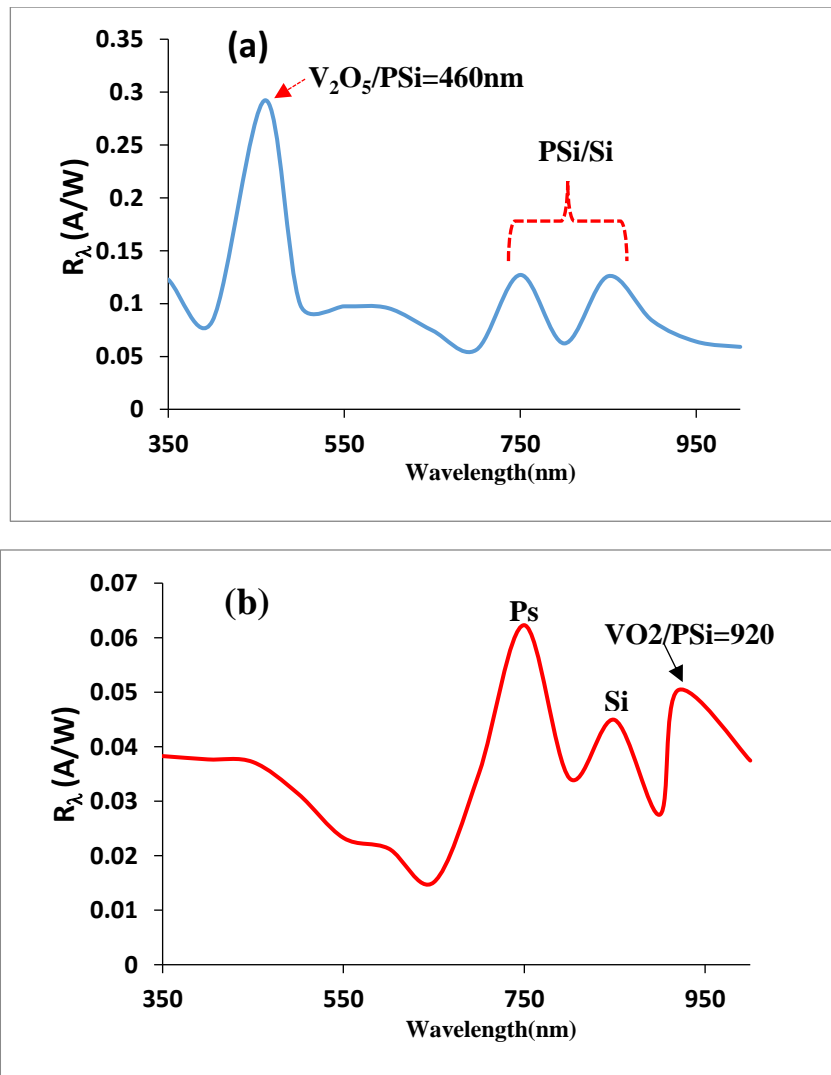
Fig. 11 (a, b) show the Specific detectivity as the function of wavelength of Ag/V2O5:PMMA/Psi/Ag and Ag/V2O5:PVP /Psi/Si/Ag structure. The Specific detectivity calculated from the relationship (6) [23] .It observed the Specific detectivity exhibits the same behavior of as the spectral responsively. The remarkable D* found to be 4.17×10^{12} W^{-1} .cm.$Hz^{1/2}$ at wavelength 460 nm for sample (a) and 8.90×10^{11} W^{-1} .cm.$Hz^{1/2}$ at wavelength750 nm for sample (b), where we notice that the sample (a) is a better photo-detector than sample (b).

$$D *= R_\lambda \frac{\sqrt{A.\Delta f}}{I_n} \qquad (5)$$

$$I_n = (2qI_d\Delta f)^{\frac{1}{2}} \qquad (6)$$

Where Δf is the bandwidth, A: active area of the detector, I_d: dark current and q: electron charge. *Fig. 11 (a, b)* show that detectivity directly related to responsiveness.
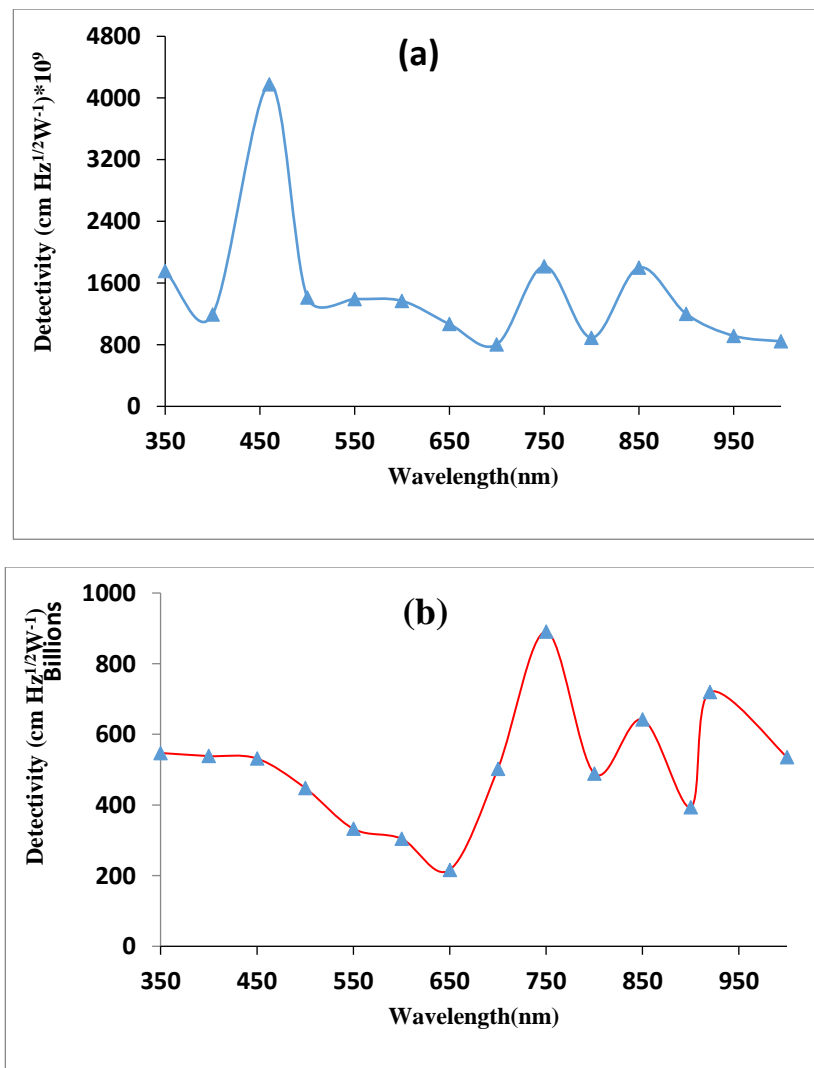
FIG. 11. SPECIFIC DETECTIVITY VS. WAVELENGTH OF (A) V2O5: PMMA/PSI/ N- SI PHOTO-DETECTORS AND (B) VO2: PVP/PSI/ N- SI PHOTO-DETECTORS.

Finally, the statistical analysis had been achieved by SPSS 24.0 window using Least Significant Difference (LSD) between varietal means to calculate a significance variation among all groups.

LSD (Least Significant Difference) is the value at particular level of statistical probability which means when exceeded by the difference between two varietal means for particular characteristic. However, the two varieties are said to be distinct for that characteristic at that or lesser.

Steps of multiple comparison between two varietal means:

1. Instruction the means descendant.
2. Definition the difference between two varietal means.
3. If the difference between them greater than LSD this indicates there is statistical significant function at the level (α= 0.05.)

After performing the binary analysis, it was found there were significant differences between varietal means for the variable the sample S and the variable wavelength λ which effect for on the variable of the responsivity R. So, it's necessary to confirm the meaning of the smallest significance difference (LSD) the results as shown in Table I. Firstly, with the respect to the variable S the smallest significant difference (LSD= 0.023):

1. (S1& S6) it is greater than the smallest LSD (0.023< 0.0233) which indicates that the difference between them statistical significant at level (α= 0.05.)

2. (S6 & S8) it is greater than the smallest LSD (0.023< 0.0605) which indicates that the difference between them statistical significant at level (α= 0.05).

3. (S3& S10) it is greater than the smallest LSD (0.**0**23< 0.0401) which indicates that the difference between them statistical significant at level (α= 0.05).

4. (S7& S10) it is greater than the smallest LSD (0.023< 0.0677) which indicates that the difference between them statistical significant at level (α= 0.05).

5. (S12& S10) it is greater than the smallest LSD (0.023< 0.0453) which indicates that the difference between them statistical significant at level (α= 0.05).

6. The difference between averages (S12& S13) it is greater than the smallest (0.023< 0.579) which indicates that the difference between them statistical significant at level (α= 0.05).

Other groups indicate that the difference between them non- statistical significant at level (α= 0.05) due to the difference was lesser than the LSD.

TABLE I. EFFECT OF SAMPLES S AND WAVELENGTHS Λ ON RESPONSIVITY R

S						S								Mean of (λ)
λ	S1	S2	S3	S4	S5	S6	S7	S8	S9	S10	S11	S12	S13	
350	0.0077	0.1227	0.0096	0.0077	0.0096	0.0402	0.1210	0.0383	0.1605	0.6919	0.0038	0.2479	0.0098	**0.1131**
400	0.0012	0.0833	0.0094	0.0075	0.0110	0.0337	0.1194	0.0377	0.1643	0.7090	0.0033	0.1831	0.0039	**0.1051**
450	0.0009	0.2923	0.0140	0.0091	0.0126	0.1202	0.1232	0.0372	0.1635	0.7384	0.0035	0.1845	0.0029	**0.1309**
500	0.0003	0.0988	0.0231	0.0069	0.0081	0.0421	0.1229	0.0313	0.1614	0.7265	0.0038	0.1710	0.0019	**0.1075**
550	0.0029	0.0974	0.0174	0.0066	0.0061	0.0467	0.1230	0.0233	0.1622	0.7309	0.0038	0.1660	0.0024	**0.1068**
600	0.0016	0.0957	0.0167	0.0067	0.0058	0.0437	0.1278	0.0213	0.1555	0.7306	0.0038	0.1627	0.0030	**0.1058**
650	0.0011	0.0746	0.0198	0.0063	0.0054	0.0523	0.1329	0.0151	0.1498	0.6772	0.0040	0.1257	0.0031	**0.0975**
700	0.0024	0.0562	0.0400	0.0073	0.0084	0.1133	0.1695	0.0352	0.2045	0.6730	0.0047	0.2323	0.0032	**0.1192**
750	0.0022	0.1271	0.0296	0.0068	0.0104	0.1144	0.1979	0.0623	0.1843	0.9163	0.0053	0.1602	0.0034	**0.1400**
800	0.0032	0.0623	0.0458	0.0070	0.0088	0.1664	0.1557	0.0342	0.2104	0.7627	0.0046	0.2355	0.0026	**0.1307**
850	0.0037	0.1259	0.0438	0.0076	0.0116	0.1433	0.1602	0.0449	0.1955	0.9023	0.0056	0.1734	0.0023	**0.1400**
900	0.0006	0.0838	0.0370	0.0069	0.0077	0.1064	0.1530	0.0275	0.2186	0.8795	0.0048	0.1709	0.0000	**0.1305**
930	0.0006	0.0640	0.0253	0.0068	0.0074	0.0890	0.1627	0.0503	0.2343	0.9916	0.0063	0.2899	0.0000	**0.1483**
1000	0.0002	0.0590	0.0233	0.0067	0.0050	0.0890	0.1349	0.0375	0.2119	0.8745	0.0037	0.1362	0.0000	**0.1217**
Mean of S	**0.0020**	**0.1031**	**0.0253**	**0.0071**	**0.0084**	**0.0858**	**0.1432**	**0.0354**	**0.1841**	**0.7860**	**0.0044**	**0.1885**	**0.00275**	**0.1212**

IV. CONCLUSIONS

In conclusion, it is a simple method to dissolve vanadium or its oxides in water, and it is simple way to dissolve polyvinylpyrrolidone (PVP) in the ethanol by using room temperature and stirring the mixture. On the other hand, due to the fact that polymethyl methacrylate (PMMA) does not agglomerate at the bottom, this can only be accomplished in the case of PMMA by using a relatively strong solvent, such as acetone, along with constant stirring of the solution. Specified the temperature does not exceed 60 degrees Celsius to prevent the occurrence of a glass transition to the material, the drop casting method is thought of as a simple and easy method that is also of high economic quality. It is very suitable for creating regular and homogeneous films. Both of the prepared compositions improved the properties of the porous silicon and demonstrated the viability of the material for use as a detector in the ultraviolet radiation region as the detection increased to 10^{11} W^{-1} $.cm.Hz^{1/2}$, and at NIR radiation region increased to 10^{13} W^{-1} $.cm.Hz^{1/2}$ at wavelength > 850 nm.

REFERENCES

[1] Adavallan, K., Krishnakumar, N.: Mulberry leaf extract mediated synthesis of gold nanoparticles and its anti-bacterial activity of against human pathogens. Adv. Nad. Sci. Nanosci. Nanotechnol. **5,** 025018 (2014).

[2] Chuah, R., Gopinath, S.C.B., Anbu, P., Salimi, M.N., Yaakub, A.R.W., Lakshmipriya, T.: Synthesis and characterization of reduced graphene oxide using the aqueous extract of *Eclipta prostrata.* 3 Biotech. **10,** 364 (2020).

[3] Ramanathan, S., Gopinath, S.C.B., Md Arshad, M.K., Poopalan, P., Anbu, P., Lakshmipriya, T.: Aluminosilicate nano-composites from incinerated Chinese holy joss fly ash: a potential nanocarrier for drug cargos. Sci. Rep. **10,** 3351 (2020).

[4] Markov, A., Greben, K., Mayer, D., Offenhäusser, A., & Wördenweber, R. In Situ Analysis of the Growth and Dielectric Properties of Organic Self-Assembled Monolayers: A Way to Tailor Organic Layers for Electronic Applications. *ACS applied materials & interfaces,* 8, 16451-16456, (2016).

[5] Sahatiya, P., & Badhulika, S. Discretely distributed 1D V 2 O 5 nanowires over 2D MoS2 nanoflakes for an enhanced broadband flexible photodetector covering the ultraviolet to near infrared region. *Journal of Materials Chemistry C*, 5, 12728-12736,(2017).

[6] Khandaker, J. I., Tokuda, M., Ogata, Y., Nishiyama, T., & Mashimo, T. Formation of Vanadium Oxide (VO System) Graded Compounds under Strong Gravitational Field *May Defect & Diffusion Forum* in (2015).

[7] Vijayakumar, Y., Jyothi, D. S., Nagaraju, P., & Reddy, M. V. Structural, electrical and optical properties of spray deposited V2O5 thin films on glass substrates. Physics and Chemistry of Glasses-European Journal of Glass Science and Technology Part B, (2016).

[8] Majid SS, Shukla DK, Rahman F, Khan S, Gautam K, Ahad A, et al. Insulator-metal transitions in the T phase Cr doped and M1 phase undoped VO2 thin films. Physical Review B.;98:075152. DOI: 10.1103/ PhysRevB.98.075152, (2018).

[9] Li M, Magdassi S, Gao Y, Long Y. Hydrothermal synthesis of VO2 polymorphs: Advantages, challenges and prospects for the application of energy efficient smart windows. Small.;13:1701147. DOI: 10.1002/ smll.201701147, (2017).

[10] W.Budde, "Physical Detector of Optical Radiation", Optical Radiation Measurements, Vol.4, , Academic Press, (1983).

[11] U. M. Nayef and M. W. Muayad, "Typical of Morphological Properties of Porous Silicon", International Journal of Basic and Applied Sciences IJBASIJENS Vol.13, No.02, (2013).

[12] H. S. Mavi, B. G. Rasheed, A K Shukla, S. C. Abbi and K. P. Jain, "Spectroscopic Investigations of Porous Silicon Prepared by Laser-Induced Etching of Silicon", J. Appl. Phys., Vol. 34, No.3, pp. 292, (2001).

[13] Raheem G. Kadhim , Raid A. Ismail ,* and Wasna'a M. Abdulridha "Structural, Morphological, Chemical and Optical Properties of Porous Silicon Prepared By Electrochemical Etching" Int. J. Thin. Fil. Sci. Tec. 4, No. 3, 199-203 (2015).

[14] K. M. Shafeeq · V. P. Athira1 · C. H. Raj Kishor · P. M. Aneesh,"Structural and optical properties of V2O5 nanostructures grown by thermal decomposition technique", Applied Physics A 126:586, (2020).

[15] Xiaowei Zhou, Guangming Wu, Jiandong Wu, Huiyu Yang, Jichao Wang and Guohua Gao*,"Carbon black anchored vanadium oxide nanobelts and their post-sintering counterpart (V2O5 nanobelts) as high performance cathodmaterials for lithium ion batteries", Phys.Chem.Chem.Phys., 16, 3973. (2014).

[16] Krystyna Schneider and Wojciech Maziarz,"V2O5 Thin Films as Nitrogen Dioxide Sensors", Proceedings ,2, 759, (2018,).

[17] Yifu Zhang,"VO2(B) conversion to VO2(A) and VO2(M) and their oxidation resistance and optical switching properties", Materials Science-Poland, 34(1), pp. 169-176,(2016).

[18]   Krystyna Schneider ,"Optical properties and electronic structure of V2O5, V2O3 and VO2 ", Journal of Materials Science: Materials in Electronics ,31:10478–10488, (2020).

[19]   A. Boutlala, F. Bourfaa, M. Mahtili, A. Bouaballou, Deposition of Co-doped TiO2 thin films by sol–gel method. IOP Conf. Ser. Mater. Sci. Eng. 108, 12048 (2016).

[20]   Manil Kang, Sok Won Kim, Younghun Hwang, Youngho Um, and Ji-Wook Ryu"Temperature dependence of the interband transition in a V2O5 film" AIP ADVANCES 3, 052129 (2013).

[21]   Krystyna Schneider ,"Optical properties and electronic structure of V2O5, V2O3 and VO2 ", Journal of Materials Science: Materials in Electronics 31:10478–10488, (2020).

[22]   Ovais M, Nadhman A, Khalil AT,. Biosynthesized colloidal silver and gold nanoparticles as emerging leishmanicidal agents: an insight. Nanomed.;12:2807 2819, (2017).

[23]   R.A. Ismail, W.K. Hamoudi, and K.K. Saleh, "Effect of rapid thermal annealing onthe characteristics of amorphous carbon/n-type crystalline silicon heterojunctionsolar cells", Materials Science in Semiconductor Processing, 21,194, (2014).

[24]   The Techniques of Based Internet Key Exchange (IKE) Protocol to Secure Key Negotiation. Iraqi Journal of Computers, Communications, Control and Systems Engineering, 22(3), 147-154. (2022).

[25]   Intelligent Parameter Tuning using Deep Q-network in Adaptive Queue Management Systems. Iraqi Journal of Computers, Communications, Control and Systems Engineering, 22(3), 62-71. (2022).

[26]   Ali, M. A., & Alsaidi, B. K. Luminance pyramid for image generation and colorization. Periodicals of Engineering and Natural Sciences, 8(2), 784-789. (2020).

[27]   Al-Selmi, A. D. H., Fenjan, F. H., & Al-Rubaye, S. A. J. Effect of taking some of dietary supplements according to special forces exercises to develop some physical abilities, speed and accuracy smash shot for badminton young players. (2019).

[28]   Al-Selmi, A.-S. The effect of continuous training on myoglobin muscle and on some specific fitness elements and bassic skills of badminton players. sprig conference (pp. 435-441). spain: journal of human sport and exercise. (2019).

[29]   Intelligent Parameter Tuning using Deep Q-network in Adaptive Queue Management Systems. Iraqi Journal of Computers, Communications, Control and Systems Engineering, 22(3), 62-71. (2022).